


# Cholesterol-induced deformation of the gramicidin-A channel inhibiting potassium ion binding and transport

Pan Xiao(肖盼), Yu Cao(曹宇), Jin Zhu(朱瑾), and Qing Liang(梁清)
**Citation:**Chin. Phys. B, 2024, 33 (**5**): 058701. DOI: 10.1088/1674-1056/ad334e

**What follows is a list of articles you may be interested in**

---

## Molecular dynamics simulations on the interactions between nucleic acids and a phospholipid bilayer

Yao Xu(徐耀), Shu-Wei Huang(黄舒伟), Hong-Ming Ding(丁泓铭), and Yu-Qiang Ma(马余强)
Chin. Phys. B, 2024, 33 (**2**): 028701. DOI: 10.1088/1674-1056/ad1178

## Coarse-grained simulations on interactions between spectrins and phase-separated lipid bilayers

Xuegui Lin(林雪桂), Xiaojie Chen(陈晓洁), and Qing Liang(梁清)
Chin. Phys. B, 2021, 30 (**6**): 068701. DOI: 10.1088/1674-1056/abf129

## Tail-structure regulated phase behaviors of a lipid bilayer

Wenwen Li(李文文), Zhao Lin(林召), Bing Yuan(元冰), and Kai Yang(杨恺)\ccclink
Chin. Phys. B, 2020, 29 (**12**): 128701. DOI: 10.1088/1674-1056/abad20

## Effect of $C_{60}$ nanoparticles on elasticity of small unilamellar vesicles composed of DPPC bilayers

Tanlin Wei(魏坦琳), Lei Zhang(张蕾), Yong Zhang(张勇)
Chin. Phys. B, 2020, 29 (**4**): 048702. DOI: 10.1088/1674-1056/ab7d9f

## Combined effects of headgroup charge and tail unsaturation of lipids on lateral organization and diffusion of lipids in model biomembranes

Xiao-Jie Chen(陈晓洁), Qing Liang(梁清)
Chin. Phys. B, 2017, 26 (**4**): 048701. DOI: 10.1088/1674-1056/26/4/048701

---

# Cholesterol-induced deformation of the gramicidin A channel inhibiting potassium ion binding and transport

Pan Xiao(肖盼)[1,2], Yu Cao(曹宇)[1,2], Jin Zhu(朱瑾)[1,2], and Qing Liang(梁清)[1,2,†]

[1] *Center for Statistical and Theoretical Condensed Matter Physics & Department of Physics, Zhejiang Normal University, Jinhua* 321004, *China*
[2] *Zhejiang Institute of Photoelectronics & Zhejiang Institute for Advanced Light Source, Zhejiang Normal University, Jinhua* 321004, *China*

(Received 4 February 2024; revised manuscript received 26 February 2024; accepted manuscript online 13 March 2024)

Gramicidin A (gA) is a kind of antibiotic peptide produced by *bacillus brevis* and it can dimerize across lipid bilayers to form a monovalent cation channel. In this work, we investigate the impact of cholesterol in the lipid bilayer on the binding of potassium ions with the gA channel and the transport of the ions across the channel. The results indicate that cholesterol can significantly influence the conformational stability of the gA channel and cause the channel deformation which inhibits the potassium ion binding with the channel and transport across the channel. The work provides some molecular insights into understanding of influence of lipids on the activity of gA channel in both model membranes and plasma membranes of intact cells.

**Keywords:** gramicidin A, lipid bilayer, molecular dynamics, interaction

**PACS:** 87.14.ef, 87.16.D–, 87.15.ap, 87.15.K– **DOI:** 10.1088/1674-1056/ad334e

## 1. Introduction

Gramicidin A (gA) is a linear antimicrobial peptide and produced by bacillus brevis.[1,2] In biomedicine, gA not only serves as antibiotics against gram-positive bacteria but also functions as therapeutic agents for cancer.[3–11] Composed of 15 alternating L- and D-amino acids, gA can form either a single-stranded helical dimer in a head-to-head manner or a double-stranded intertwined helix in model membrane,[2,12] depending on the property of the solvent in which gA is dissolved before incorporated into the lipid bilayer.[13,14] The single-stranded gA dimer with a larger radius can transport monovalent cations such as potassium ions ($K^+$) and sodium ions ($Na^+$) whereas the double-stranded one is considered a non-channel conformation.[1,2] Due to its simple structure, gA is an ideal model for studying the conformation, dynamics, and functions of ion channel in the plasma membrane of intact cells and for synthesis of artificial ion channels for biomedical applications.[1,15–17]

The conformation of gA channel is unstable and shows a high sensitivity to its environments, which is highly involved in the formation and ion-transport activity of the channel. It has been shown that the membrane spontaneous curvature or the membrane deformation induced by the hydrophobic mismatch effect is a key factor influencing the dimerization or lifetime of gA channel, and the large curvature or deformation of membrane could hinder the formation of gA channel.[18–22] Recently, Foreman-Ortiz *et al.* found that the local deformation of the lipid bilayer perturbed by an anionic nanoparticle may reduce the activity but extend the lifetime of gA channel.[23] In a supported lipid bilayer, Su *et al.* indicated that a negative transmembrane potential can reduce a tilt angle of gA channel and thus facilitate the cation transport across the channel.[24] Furthermore, once two gA channels are connected by a linker, their lifetime will be significantly increased.[25–27]

Cholesterol (CHOL), as a major lipid component of plasma membranes of mammalian cells, exhibits significant impact on the conformation and activity of a variety of ion channels.[28–34] For gA, some experimental studies have shown that gA channel inactivation occurs in CHOL-containing erythrocyte membranes and the rate of channel inactivation is strongly dependent on the phospholipid-to-CHOL molar ratio in the membrane.[35,36] The reduction in ion selectivity of gA channel requires that one gA interacts with at least five CHOL molecules, while the activity of gA channel is likely unaffected if the amount of CHOL in the membrane is low. Besides the direct interaction of CHOL with gA, CHOL can also influence the formation of gA channel through regulating the lateral packing and mobility of lipids as well as the bilayer thickness.[37,38] However, the molecular mechanism of the effect of CHOL on the function of ion transport of gA channel remains elusive.

In this study, we systematically investigate the effects of CHOL on the interactions of $K^+$ ions with gA channel in model membranes by employing the all-atom molecular dynamics (MD) simulations. We examine the binding of $K^+$ ions with gA channel in the model membranes with varying CHOL concentration using the unbiased MD simulation. The results indicate that the increase of CHOL in the membrane results in the deformation of the gA channel and inhibits the binding of $K^+$ ions with the channel. Furthermore, using biased MD simulations, we calculate the transferring free energy of a $K^+$

†Corresponding author. E-mail: qliang@zjnu.edu.cn

© 2024 Chinese Physical Society and IOP Publishing Ltd 

ion from the binding site at the entrance of the gA channel to the center of the channel in the lipid bilayers with different CHOL concentrations, and energetically reveal the influence of CHOL on the transport of $K^+$ ion across the channel.

## 2. Model and methods

### 2.1. System setup

In this work, we focus on the effect of CHOL on the interactions of $K^+$ ions with gA channel. According to the relevant experimental system,[35] we built the lipid bilayers using dimyristoylphosphatidylcholine (DMPC) and CHOL with varying molar ratios. We considered three lipid bilayers: one unitary bilayer composed of pure DMPC, and two binary bilayers composed of DMPC and CHOL with molar ratios of 8 : 2 and 6 : 4, respectively. The molar concentration of CHOL in the three lipid bilayers are 0 mol%, 20 mol%, and 40 mol%, respectively. A channel of gA dimer (PDB:1JNO) was inserted into the lipid bilayers. Each lipid bilayer was solvated by about 9100 TIP3P water molecules, and 0.15 M potassium chloride (KCl) was added to the system. All the systems were built using the membrane builder module of the web-based tool CHARMM-GUI (www.charmm-gui.org).[38–41] Figure 1 shows the molecular structures of the lipids, a gA channel and a lipid bilayer consisting of DMPC and CHOL inserted with a gA channel.

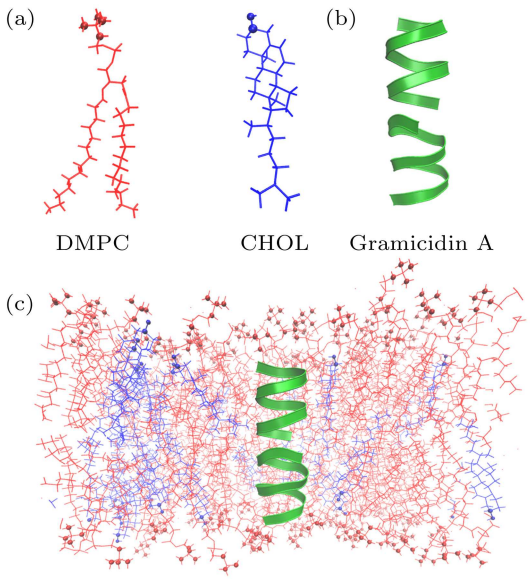



**Fig. 1.** (a) The molecular structures of DMPC and CHOL with their headgroups displayed with beads. (b) Illustration of a gA channel shown with ribbons. (c) A lipid bilayer composed of DMPC and CHOL, inserted with a gA channel.

### 2.2. All-atom MD simulations

In this paper, all systems were simulated by using all-atom MD simulations, and the CHARMM36 force field was adopted for the simulations.[42–44] The simulations were performed with GROMACS (version 2020.4) package.[45,46] The ensemble of constant particle number, pressure, and temperature (NPT) was used for the simulations. The temperature was maintained at 303.15 K by the velocity-rescaling temperature coupling scheme with a time constant of 1 ps,[47] and the pressure was controlled at 1.0 bar by a Parrinello–Rahman semi-isotropic barostat with a time constant of 3 ps.[48] The long-ranged electrostatic interaction was calculated using the particle mesh Ewald (PME) method and the nonbonded Lennard–Jones interaction was cut off at 1.1 nm.

Each simulation was run for 500 ns with a 2-fs time step after energy minimization and equilibrium simulations, and five copies of simulations with different initial conditions were performed for each system to guarantee the validity of the results. The initial size of the simulation box is about $8 \times 8 \times 8.5$ nm$^3$, and the periodic boundary conditions were applied in all three directions.

### 2.3. Calculation of the potential of mean force

Besides the unbiased simulations, to estimate the free energy barrier of the transport of $K^+$ ions across the gA channel in the lipid bilayers with different CHOL concentrations, the biased simulations were also performed to calculate the potential of mean force (PMF) of the $K^+$ ion transferring from the binding site W15 at the entrance of the gA channel to the center of the channel using the umbrella sampling technique. We took the state that the $K^+$ ion binds to W15 of the gA channel in the unbiased simulations as the initial state for calculating the PMF between the $K^+$ ion and the gA channel and pulled the $K^+$ ion from the W15 residue of gA to the center of the channel using a pull MD simulation. It is notable that, during pulling of the $K^+$ ion, gA channel may undergo a dramatic deformation and the ion may be pulled out of the channel. To avoid the occurrence of this case, one should carefully check the initial state of each sampling window to ensure that the ion locates in the channel in all the windows. Once ion is pulled out of the channel in one or more windows, the pull simulation should be restarted with a different initial condition. A total of 12 sampling windows were generated with an interval of 0.1 nm along the $z$-direction, ranging from 0 to 1.2 nm from the $K^+$ ion binding site at the entrance of gA channel to the center of mass (COM) of the gA dimer. In each window, the position of the $K^+$ ion was restrained by a harmonic potential with a force constant of 1000 kJ·mol$^{-1}$·nm$^{-2}$. Each window was simulated for 50 ns, and the trajectory was used for calculating the PMF with the weighted histogram analysis method using the program gmx wham in GROMACS package,[49,50] and the convergence and error were estimated.[51]

### 2.4. Data analysis

The visualization of MD trajectories was realized by the software of Visual Molecular Dynamics (VMD).[52] The contact frequency (number of contacts per nanosecond) of $K^+$

ions/CHOL with gA channels as well as the number of contacts of $K^+$ ion with its binding site at the entrance of gA channel were calculated using the gmx mindist tool in GROMACS with a cut-off distance of 0.4 nm. The root-mean-square deviation (RMSD) of gA was calculated using the tool gmx rms in GROMACS to estimate the conformational stability of gA channel. The number of hydrogen bonds between the two monomers of the gA channel was analyzed using *gmx hbond* with a cut-off distance of 0.4 nm. The thickness of lipid bilayer and the length of gA were obtained using the MDAnalysis package.[53] Here, the lipid bilayer thickness was measured by the distance between the nitrogen (N) atoms in the headgroups of DMPC lipids in the two leaflets of lipid bilayer, and the gA length was defined by the distance between the tryptophan residues W15 and W30 at the ends of the two monomers in the two leaflets of the bilayer.

## 3. Results and discussion

### 3.1. $K^+$ ions binding with gA channel in lipid bilayers with varying CHOL concentration

Figure 2 shows the dynamic processes of $K^+$ ions interacting with the gA channel in the lipid bilayers composed of pure DMPC (0 mol% CHOL), 8 : 2 DMPC/CHOL (20 mol% CHOL), and 6 : 4 DMPC/CHOL (40 mol% CHOL). The results exhibit that, in all the three systems, one of the $K^+$ ions binds at the entrance of the gA channel at $\sim$ 200 ns. It is notable that, although there are many $K^+$ ions in the systems, only one $K^+$ ion is observed to bind to the gA channel throughout the whole simulation time.

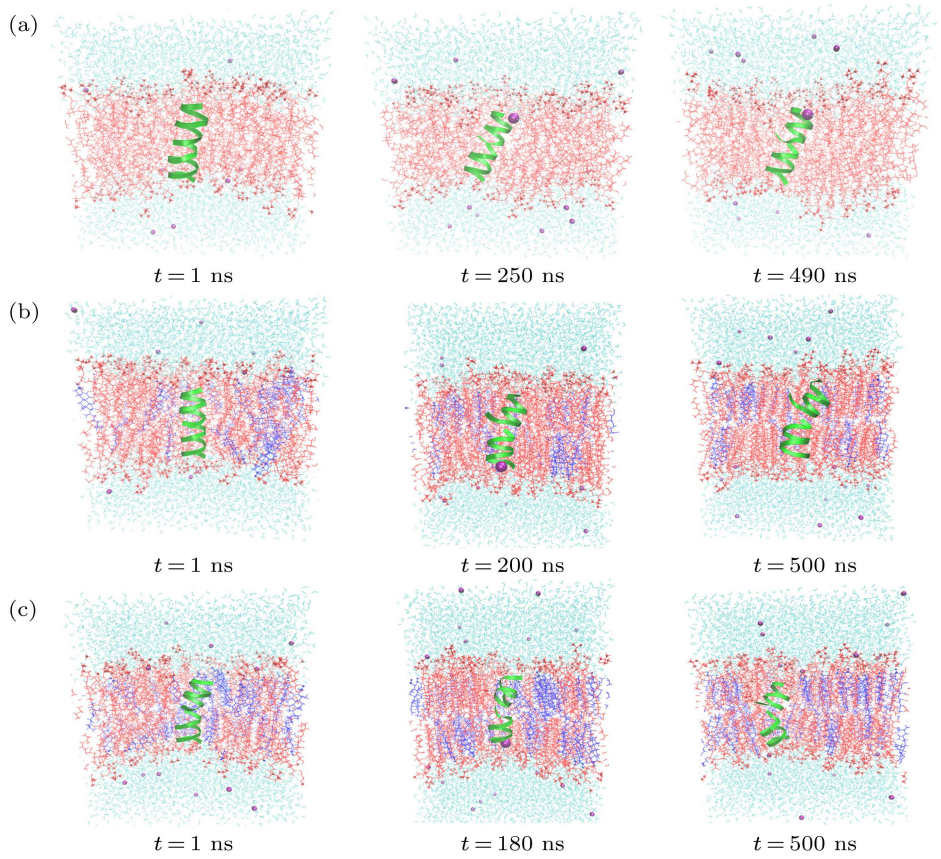



**Fig. 2.** Dynamic process of $K^+$ ions (purple) interacting with the gA channel in the lipid bilayers composed of (a) pure DMPC, (b) 8 : 2 DMPC/CHOL, and (c) 6 : 4 DMPC/CHOL, respectively. For clarity, the $K^+$ ion binding at the entrance of the gA channel is shown with a larger size. The water molecules are shown in light blue.

However, the binding stabilities of $K^+$ ions in the three systems are different. In the lipid bilayer composed of pure DMPC, the $K^+$ ion stably binds with the gA channel in most of the time within the stage of 200–500 ns of the simulation as shown in Fig. 2(a). In the other two systems, the $K^+$ ion binds to the gA channel unstably within the period of 200–500 ns of simulations and it separates from the binding site at the end of the simulations as shown in Figs. 2(b) and 2(c). Additionally, in the two CHOL-containing systems, the conformation of the gA channel exhibits an extreme deformation. In all the three systems, neither the $K^+$ ion entering the channel nor transport across the channel was observed due to the limitation of the short time length of the simulations.

We further calculated the contact frequency of the $K^+$ ions with gA channel in the three systems and the contact frequency of CHOL with gA in the CHOL-containing lipid bilayers (Fig. 3). With increasing the CHOL concentration, the contact frequency of $K^+$ ions with gA channel obviously decreases while the contact frequency of CHOL with gA in-

creases, indicating that CHOL strongly interacts with the gA channel and hinders the contacts between $K^+$ ions and gA channel.

To determine the binding sites of $K^+$ ions with the gA channel, we calculated the contact frequency of the $K^+$ ion with individual residues in gA, and the results are shown in Fig. 4. The main residues involved in $K^+$ ion binding include W11, L12, W13, L14, and W15 of gA. The $K^+$ ions contact with the residues of L12 and L14 with a relatively high frequency, but the highest contact frequency appears at the residue of W15. Thus, our simulations indicate that the most possible binding site for $K^+$ ion with gA channel is the W15 (or W30) residue at the entrance of the channel. In the previous experimental studies, it was also found that the binding site of $K^+$ ion is near the entrance of the gA channel and W15 is the most possible binding residue.[54,55] Therefore, our results are consistent with the experimental results.

Figure 5 further shows the number of contacts of $K^+$ ions with the binding site of W15 (or W30) at the gA entrance versus the simulation time. In the pure DMPC bilayer (0 mol% CHOL), $K^+$ ions contact the binding site frequently in the last 300 ns of the whole simulation as shown in Fig. 5(a). In the other systems containing 20 mol% and 40 mol% CHOL, respectively, the number of contacts between $K^+$ ions and the binding site becomes much less than that in the pure DMPC bilayer and it reduces with the increase of the CHOL concentration [Figs. 5(b) and 5(c)]. Thus, the contacts of $K^+$ ions with the binding site are unstable throughout the whole 500 ns simulations in the CHOL-containing lipid bilayers.

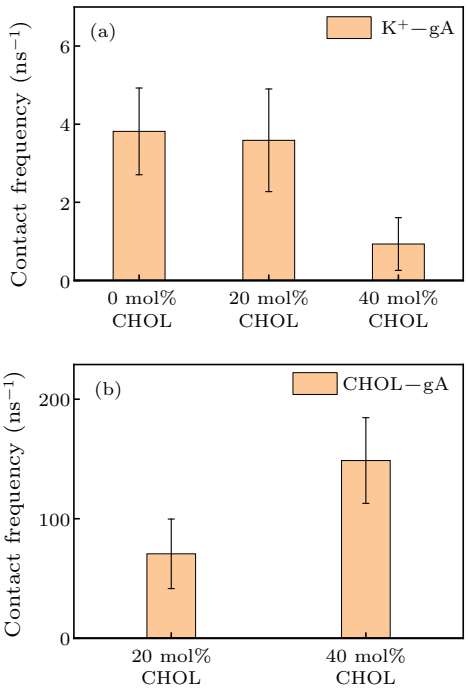



**Fig. 3.** Time-averaged contact frequencies of (a) $K^+$ ions with the gA channel and (b) CHOL with the gA channel in the lipid bilayer with different CHOL concentrations in the last 50 ns of the simulations.

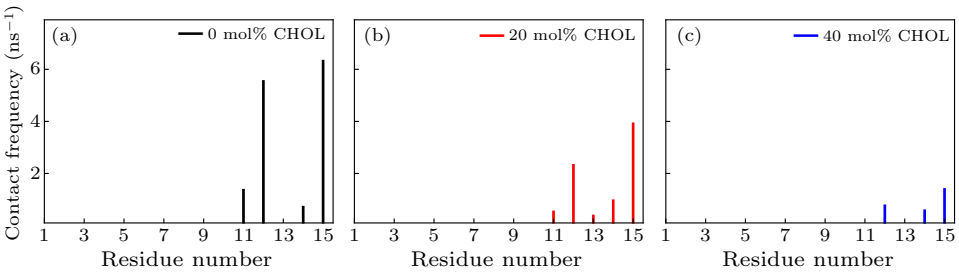



**Fig. 4.** Contact frequency of $K^+$ ions with the individual residues of gA in the lipid bilayers composed of (a) pure DMPC, (b) 8 : 2 DMPC/CHOL, and (c) 6 : 4 DMPC/CHOL, respectively.

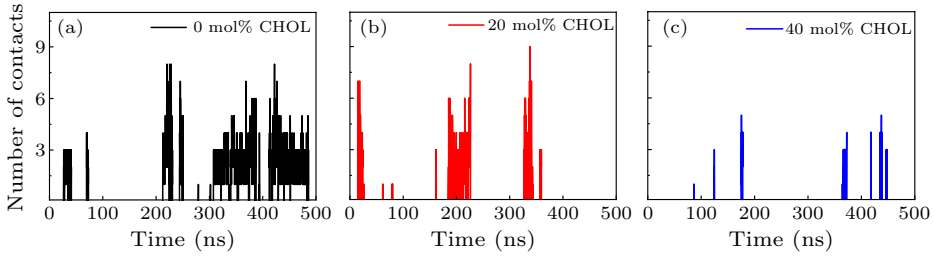



**Fig. 5.** Number of contacts between $K^+$ ions with the tryptophan residue (W15) at the entrance of gA channel in the lipid bilayer composed of (a) pure DMPC, (b) 8 : 2 DMPC/CHOL, and (c) 6 : 4 DMPC/CHOL, respectively.

To further explore the influence of CHOL on the deformation of gA channel, we compared the RMSD of the gA dimer in the three systems as shown in Fig. 6(a). We find that, in the pure DMPC lipid bilayer, the gA dimer maintains a relatively stable conformation with the RMSD of $\sim 0.15$ nm. In the other two systems containing CHOL, the RMSD of the gA dimer is obviously larger than that in the pure DMPC lipid bilayer, which indicates that CHOL can lead to the conformational instability of the gA channel. Interestingly, the conformation of gA channel does not become more unstable with the

increase of CHOL concentration. On the contrary, the RMSD of gA channel in the lipid bilayer containing 20 mol% CHOL exceeds the RMSD of gA in the lipid bilayer with 40 mol% CHOL in the later stage of the simulations.

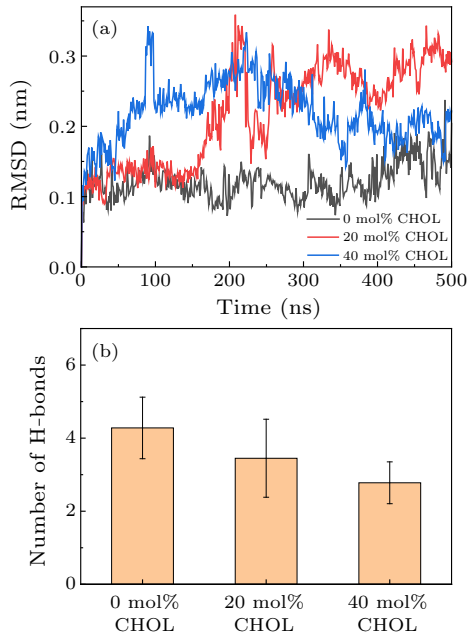



**Fig. 6.** (a) RMSD of the gA channel in the lipid bilayers with different CHOL concentrations. (b) Time-averaged number of hydrogen bonds between the two monomers of the gA channel in the lipid bilayers with different CHOL concentrations in the last 50 ns of the simulations.

In the gA channel, two monomers are connected by hydrogen bonds. The number of hydrogen bonds between the two monomers determines the conformational stability of the channel. Figure 6(b) presents the number of hydrogen bonds between the two monomers of the gA channel in the lipid bilayers with different CHOL concentration. It is shown that, with increasing CHOL concentration, the number of hydrogen bonds between the two monomers of the channel reduces monotonously. This result further indicates that the increase of CHOL concentration in the lipid bilayer causes the rupture of the hydrogen bonds between the two monomers of the gA channel and results in the significant deformation of the channel.

Figure 7 shows the length of the gA channel and the difference between the bilayer thickness and the channel length in the lipid bilayers with different CHOL concentration. We find that, with the increase of the CHOL concentration, the length of the channel reduces. Contrarily, the bilayer thickness which is denoted by the total height of the histogram in Fig. 7 is increased by CHOL. Therefore, the mismatch between the thickness of the lipid bilayer and the length of the gA channel becomes stronger with increasing CHOL concentration. In the lipid bilayer with higher CHOL concentration (e.g., 40 mol%), the whole gA channel is embedded in the hydrophobic part of the lipid bilayers and the $K^+$ ions are difficult to spontaneously penetrate the hydrophobic part of the lipid bilayer. Therefore, the contacts between the ions and the channel decreases with the increase of CHOL concentration as shown in Figs. 4 and 5.

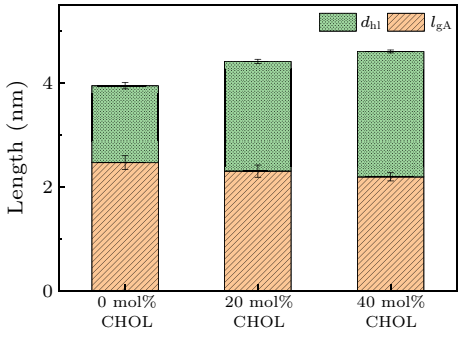



**Fig. 7.** Time-averaged length ($l_{gA}$) of the gA channel and the difference ($d_{hl}$) between the bilayer thickness and the channel length in the three lipid bilayers with different CHOL concentrations in the last 50 ns of the simulations.

### 3.2. Influence of CHOL on the $K^+$ ion transport across gA channel

As mentioned above, we did not observe either the spontaneous entering of $K^+$ ions into the gA channel or transporting across the channel in the unbiased simulations because of the limitation of the simulation time length. To estimate the influence of CHOL on the transport of $K^+$ ions across gA channel, we pulled a $K^+$ ion from the binding site W15 at the entrance of the channel to the center of the channel through the biased simulations and calculated the PMF profiles as shown in Fig. 8. The difference of the PMF at the channel center (the COM distance of 0 nm) and the PMF at the binding site (the COM distance of 1.2 nm) is the free energy barrier that the $K^+$ ion needs to overcome as it enters the channel.

The results indicate that, with increasing CHOL concentration, the free energy barrier of the ion entering the channel decreases. In the pure DMPC bilayer, the free energy barrier is high, the $K^+$ ion binds with W15 tightly and is relatively difficult to separate from the binding site to enter the channel. With increasing CHOL concentration, the $K^+$ ion separates from the binding site and enters the channel more easily indicated by the lower free energy barriers. It is notable that we do not consider the process of the $K^+$ ion penetrating the lipid bilayer from the solution and binding with gA channel. Due to the hydrophobic interaction, the $K^+$ ion is difficult to spontaneously penetrate the bilayer and bind with the gA channel which is completely embedded in the hydrophobic part of the bilayer as shown in Figs. 2 and 6. Thus, the PMF profiles only imply that CHOL facilitates the $K^+$ ion entering the gA channel from the binding site at the entrance of the channel, but do not indicate that CHOL can promote the transport of the $K^+$ ions across the lipid bilayer since the ions have to penetrate a hydrophobic layer before binding with W15 of the channel in the CHOL-containing lipid bilayers.

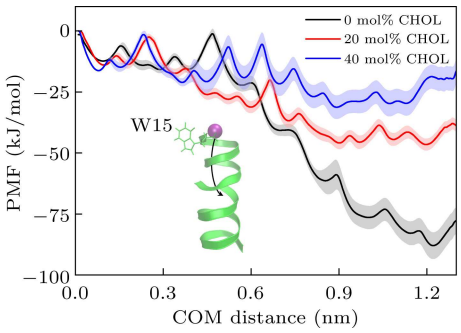



**Fig. 8.** PMF profiles of a $K^+$ ion transferring from the binding site of W15 residue at the entrance of the gA channel to the COM of the channel. Here, the COM distance of 0 nm corresponds to the center of the channel, and the COM distance of 1.2 nm corresponds to W15 residue at the channel entrance. The inset illustrates the pulling pathway of the $K^+$ ion from the binding site to the COM of the gA channel. The errors are shown with shadows.

The previous experiments indicated that CHOL may inhibit the transport of $K^+$ ions across the gA channel but the microscopic mechanism is not very clear.[35,36] The PMF profiles shown in Fig. 8 indicate that the CHOL-induced inhibition of $K^+$ ion transport across gA channel may not be attributed to the direct CHOL-gA interaction which facilitates the ions entering the channel from the binding site W15 of gA. CHOL enhances the mismatch between the length of the channel and the thickness of the lipid bilayer and hinders the contacts between the ions and gA channel, leading to the reduction of the probability of the transport of $K^+$ ions across the channel. Additionally, the relevant experiment also showed that the well-defined conformation of the gA channel is crucial for the transport of $K^+$ ion across the channel, and the activity of gA channel may be destroyed if the channel is deformed.[56] As shown in Figs. 2 and 6, with the increase of CHOL concentration in the lipid bilayer, the gA channel is deformed extremely, which deactivates the gA channel for the transport of the $K^+$ ion. Therefore, our results agree well with the experimental result.

## 4. Conclusions

Using both unbiased and biased MD simulations, we have investigated the influence of CHOL in the lipid bilayer on the interactions between $K^+$ ions and gA channel from the molecular scale. The results indicate that CHOL can increase the thickness of the lipid bilayer but reduce the length of the gA channel through deforming the conformation of the gA channel. Thus, the mismatch between the lipid bilayer and the gA channel increases in the CHOL-containing lipid bilayers, and the gA channel is completely embedded in the hydrophobic part of the lipid bilayer, which inhibits the $K^+$ ion binding with gA channel as well as the transport of the ions across the channel, leading to dysfunction of gA channel. However, once the $K^+$ ion binds with the binding site at the entrance of gA channel, CHOL can promote the ions entering the channel. The findings are consistent well with the experiments and provide some molecular insights into understanding the transport of $K^+$ ions across the gA channel in the plasma membrane of intact cell.

Additionally, our results reveal that, as an antimicrobial peptide, gA exhibits selectivity towards most bacteria over eukaryotic cells, possibly due to the absence of CHOL in bacterial membranes. In the medical applications, for combating the rare bacteria (e.g., borrelia or helicobacter) whose membranes contain CHOL,[57] it is advisable to refrain from using gA as a candidate antimicrobial agent. Also, when utilized an anticancer agent, some modification of gA might be necessary to enhance its activity by reducing its interaction with the cholesterol in the plasma membranes of cancer cells.

## Acknowledgments

Project supported by the National Natural Science Foundation of China (Grant No. 11674287) and the Zhejiang Provincial Natural Science Foundation of China (Grant No. LY19A040009). Computational resources provided by the Scientific Computation Center of Zhejiang Normal University are greatly appreciated.

## References

[1] Kelkar D A and Chattopadhyay A 2007 *Biochim. Biophys. Acta Biomembr.* **1768** 2011
[2] Veatch W R, Fossel E T and Blout E R 1974 *Biochemistry* **13** 5249
[3] Yang M, Liu S and Zhang C 2023 *Curr. Res. Biotechnol.* **5** 100121
[4] Pavithrra G and Rajasekaran R 2020 *Int. J. Pept. Res. Therap.* **26** 191
[5] Zerfas B L, Joo Y and Gao J 2016 *ChemMedChem* **11** 629
[6] David J M and Rajasekaran A K 2015 *J. Kidney. Cancer. VHL* **2** 15
[7] Moretta A, Scieuzo C, Petrone A M, Salvia R, Manniello M D, Franco A, Lucchetti D, Vassallo A, Vogel H, Sgambato A and Falabella P 2021 *Front. Cell. Infect. Microbiol.* **11** 668632
[8] Haoyang W W, Xiao Q, Ye Z, Fu Y, Zhang D W, Li J, Xiao L, Li Z T and Hou J L 2021 *Chem. Commun.* **57** 1097
[9] Xue Y W, Itoh H, Dan S and Inoue M 2022 *Chem. Sci.* **13** 7482
[10] Chen T, Wang Y, Yang Y, Yu K, Cao X, Su F, Xu H, Peng Y, Hu Y, Qian F and Wang Z 2019 *Biol. Res.* **52** 57
[11] Yan T, Zheng X, Liu S, Zou Y and Liu J 2022 *Sci. China Chem.* **65** 1265
[12] Urry D 1971 *Proc. Natl. Acad. Sci. USA* **68** 672
[13] LoGrasso P, Moll F and Cross T 1988 *Biophys. J.* **54** 259
[14] Killian J A, Prasad K U, Hains D and Urry D W 1988 *Biochemistry* **27** 4848
[15] Zheng S P, Huang L B, Sun Z and Barboiu M 2020 *Angew. Chem. Int. Ed.* **60** 566
[16] Takada Y, Itoh H, Paudel A, Panthee S, Hamamoto H, Sekimizu K and Inoue M 2020 *Nat. Commun.* **11** 4935
[17] Barboiu M, Le Duc Y, Gilles A, Cazade PA, Michau M, Marie Legrand Y, van der Lee A, Coasne B, Parvizi P, Post J and Fyles T 2014 *Nat. Commun.* **5** 4142
[18] Kondrashov O V, Galimzyanov T R, Molotkovsky R J, Batishchev O V and Akimov S A 2020 *Membranes* **10** 368
[19] Sun D, He S, Bennett W F D, Bilodeau C L, Andersen O S, Lightstone F C and Ingólfsson H I 2020 *J. Chem. Theory Comput.* **17** 7
[20] Maer A M, Rusinova R, Providence L L, Ingólfsson H I, Collingwood S A, Lundbæk J A and Andersen O S 2022 *Front. Physiol.* **13** 836789
[21] Kondrashov O V, Galimzyanov T R, Pavlov K V, Kotova E A, Antonenko Y N and Akimov S A 2018 *Biophys. J.* **115** 478

[22] Yoo J and Cui Q 2013 *Biophys. J.* **104** 128

[23] Foreman-Ortiz I U, Liang D, Laudadio E D, Calderin J D, Wu M, Keshri P, Zhang X, Schwartz M P, Hamers R J, Rotello V M, Murphy C J, Cui Q and Pedersen J A 2020 *Proc. Natl. Acad. Sci. USA* **117** 27854

[24] Su Z, Goodall B, Leitch J J and Lipkowski J 2021 *Electrochim. Acta* **375** 137892

[25] Novoderezhkin V I, Rokitskaya T I, Kotova E A and Antonenko Y N 2023 *Phys. Chem. Chem. Phys.* **25** 3752

[26] Partenskii M B, Miloshevsky G V and Jordan P C 2003 *J. Chem. Phys.* **118** 10306

[27] Goforth R L, Chi A K, Greathouse D V, Providence L L, Koeppe R E II and Andersen O S 2003 *J. Gen. Physiol.* **121** 477

[28] Levitan I, Singh D K and Rosenhouse-Dantsker A 2014 *Front. Physiol.* **5** 65

[29] Corradi V, Bukiya A N, Miranda W E, Cui M, Plant L D, Logothetis D E, Tieleman D P, Noskov S Y and Rosenhouse-Dantsker A 2022 *Proc. Natl. Acad. Sci. USA* **119** e2109431119

[30] Han S, Chu X P, Goodson R, Gamel P, Peng S, Vance J and Wang S Z 2022 *Proc. Natl. Acad. Sci. USA* **119** e2205420119

[31] Borcik C G, Eason I R, Yekefallah M, Amani R, Han R X, Vanderloop B H and Wylie B J 2022 *Angew. Chem. Int. Ed.* **61** e202112232

[32] Zakany F, Kovacs T, Panyi G and Varga Z 2020 *Biochim. Biophys. Acta Mol. Cell Biol. Lipids* **1865** 158706

[33] Jin Y P, Liang Q and Tieleman D P 2020 *J. Phys. Chem. B* **124** 3054

[34] Qin X X, Tieleman D P and Liang Q 2022 *Biophys. J.* **121** 2069

[35] Schagina L V, Blasko K, Grinfeldt A E, Korchev Y E and Lev A A 1989 *Biochim. Biophys. Acta Biomembr.* **978** 145

[36] Schagina L V, Korchev Y E, Grinfeldt A E, Lev A A and Blasto K 1992 *Biochim. Biophys. Acta Biomembr.* **1109** 91

[37] Reiter R, Zaitseva E, Baaken G, Halimeh I, Behrends J C and Zumbuehl A 2019 *Langmuir* **35** 14959

[38] Patrick J W, Gamez R C and Russell D H 2016 *Biophys. J.* **110** 1826

[39] Lee J, Cheng X, Swails J M, Yeom M S, Eastman P K, Lemkul J A, Wei S, Buckner J, Jeong J C, Qi Y, Jo S, Pande V S, Case D A, Brooks III C L, Mackerell Jr. A D, Klauda J B and Im W 2016 *J. Chem. Theory Comput.* **12** 405

[40] Jo S, Klauda J B and Im W 2009 *Biophys. J.* **97** 50

[41] Jo S, Kim T, Iyer V G and Im W 2008 *J. Comput. Chem.* **29** 1859

[42] Klauda J B, Venable R M, Freites J A, O'Connor J W, Tobias D J, Mondragon-Ramirez C, Vorobyov I, MacKerell A D and Pastor R W 2010 *J. Phys. Chem. B* **114** 7830

[43] Huang J and MacKerell A D 2013 *J. Comput. Chem.* **34** 2135

[44] Pastor R W and MacKerell A D 2011 *J. Phys. Chem. Lett.* **2** 1526

[45] Van Der Spoel D, Lindahl E, Hess B, Groenhof G, Mark A E and Berendsen H J C 2005 *J. Comput. Chem.* **26** 1701

[46] Abraham M J, Murtola T, Schulz R, Páll S, Smith J C, Hess B and Lindahl E 2015 *SoftwareX* **1** 19

[47] Bussi G, Donadio D and Parrinello M 2007 *J. Chem. Phys.* **126** 014101

[48] Parrinello M and Rahman A 1981 *J. Appl. Phys.* **52** 7182

[49] Hub J S, de Groot B L and van der Spoel D 2010 *J. Chem. Theory Comput.* **6** 3713

[50] Kumar S, Rosenberg J M, Bouzida D, Swendsen R H and Kollman P A 1992 *J. Comput. Chem.* **13** 1011

[51] Zhu F Q and Hummer G 2012 *J. Comput. Chem.* **33** 453

[52] Humphrey W, Dalke A and Schulten K 1996 *J. Mol. Graph.* **14** 33

[53] Michaud-Agrawal N, Denning E J, Woolf T B and Beckstein O 2011 *J. Comput. Chem.* **32** 2319

[54] Olah G A, Huang H W, Liu W H and Wu Y L 1991 *J. Mol. Biol.* **218** 847

[55] Sham S S, Shobana S, Townsley L E, Jordan J B, Fernandez J Q, Andersen O S, Greathouse D V and Hinton J F 2003 *Biochemistry* **42** 1401

[56] Miloshevsky G V and Jordan P C 2006 *Structure* **14** 1241

[57] Huang Z and London E 2016 *Chem. Phys. Lipids* **199** 11